Chemical Engineering Science 230 (2021) 116095

Contents lists available at ScienceDirect

Chemical Engineering Science

journal homepage: www.elsevier.com/locate/ces

Surface tension as a function of temperature and composition for a broad range of mixtures ☆,☆☆

Nadia Shardt [a], Yingnan Wang [b], Zhehui Jin [b], Janet A.W. Elliott [a,*]

[a] Department of Chemical and Materials Engineering, University of Alberta, Edmonton, AB T6G 1H9, Canada
[b] School of Mining and Petroleum Engineering, Department of Civil and Environmental Engineering, University of Alberta, Edmonton, AB T6G 1H9, Canada

HIGHLIGHTS

- A new simple and highly accurate model for surface tension of mixtures is developed.
- A reduced mole fraction is introduced.
- Predictions are made for mixtures with and without a supercritical compound.
- The proposed model is tested for binary mixtures and a ternary mixture.

ARTICLE INFO

Article history:
Received 28 June 2020
Received in revised form 26 August 2020
Accepted 29 August 2020
Available online 6 September 2020

Keywords:
Surface tension
Multicomponent
Hydrocarbons
Thermodynamics
Critical composition

ABSTRACT

It is desirable to predict the surface tension of liquid mixtures for a wide range of compositions, temperatures, and pressures, but current state-of-the-art calculations (*e.g.*, density gradient theory) are computationally expensive. We propose a computationally simple—but accurate—semi-empirical mathematical model of surface tension for a wide variety of multicomponent mixtures, including those with a supercritical compound when coupled with an equation of state (by introducing a reduced mole fraction scaled by a critical composition). Our predictions for binary systems with one supercritical component are an average of 0.22 mN/m away from literature experimental data (466 data points), and those for systems with two subcritical components (293–333 K) are within 0.09 mN/m (236 data points). We make predictions for methanol + ethanol + water using binary coefficients within an average of 0.71 mN/m (196 data points). Given its computational simplicity and wide applicability, the proposed model will be useful for many applications.

1. Introduction

The way a fluid behaves—how it flows, how it rests, and how it nucleates—is influenced by the magnitude of its surface tension. The importance of an equation that describes the surface tension of multicomponent systems as a function of composition and temperature is far-reaching. A vast array of applications and fundamental phenomena involve liquid mixtures whose behavior is driven by the magnitude of surface tension. For instance, the surface tension of fluid mixtures influences how food packaging is designed (Karbowiak et al., 2006; Liu et al., 2018), how drugs are delivered (Arzhavitina and Steckel, 2010; Le Brun et al., 2000; Connors and Mecozzi, 2010; Koch et al., 2011), and how shale gas can be extracted from porous media underground (Firoozabadi, 2016; Jin and Firoozabadi, 2016; Tan and Piri, 2015a,b; Wang et al., 2014). Technologies such as micro-/nanofluidic chips (Eslami and Elliott, 2013, 2014a, 2014b; Shim et al., 2007; Wu et al., 2012) and ink-jet printers (Daehwan et al., 2009; Lee et al., 2005) also handle multicomponent mixtures. More widely, researchers in the fields of atmospheric physics (Aumann et al., 2010; Boyer and Dutcher, 2017), catalysis (Brown, 2018), heat transfer (Bastakoti et al., 2018), nucleation (Baidakov et al., 2012; Blander et al., 1971; Kuchma and Shchekin, 2019; Ward et al., 1970), and vapor–liquid phase equilibrium (Sandoval et al., 2016; Shardt and Elliott, 2016, 2018; Tan and Piri, 2015a,b), or phase change (Diddens et al., 2017; Kim and Stone, 2018; Ozturk and Erbil, 2018; Yu et al., 2019) all examine mixtures at varying temperatures. Thus, surface tension must be accurately quantified

☆ NS performed this research and composed the first draft of the manuscript under the direction and supervision of JAWE. YW and ZJ provided motivation for this work and gave assistance with PR-EOS phase equilibrium calculations for hydrocarbon mixtures. All authors contributed to the final manuscript.
☆☆ Declarations of interest: none

* Corresponding author.
E-mail address: janet.elliott@ualberta.ca (J.A.W. Elliott).

https://doi.org/10.1016/j.ces.2020.116095
0009-2509/

so that diverse phenomena can be better understood, predicted, and controlled when, for example, temperatures, pressures, and/or compositions vary.

For a pure compound's surface tension, accurate theoretical descriptions have been obtained by fitting to experimental data. The mathematical form of fitted equations in the literature ranges from a linear equation (the Eötvös equation (Eötvös, 1886)) or other algebraic forms (*e.g.*, the principle of corresponding states (Brock and Bird, 1955; Guggenheim, 1945) and the parachor model (Macleod–Sugden equation (Macleod, 1923)) to a differential equation that describes the distribution of molecules through the interfacial region (*e.g.*, density gradient theory (Breure and Peters, 2012; Cahn and Hilliard, 1958; Cornelisse et al., 1993; Lin et al., 2008; Miqueu et al., 2005; Van der Waals, 1979) or density functional theory (Gloor et al., 2007; Li and Firoozabadi, 2009; Tang and Gross, 2010) combined with a Helmholtz free energy approximation to calculate interfacial properties).

A similarly broad range of approaches has been investigated to describe how surface tension varies as a function of composition. Simpler models include the parachor model (Weinaug–Katz equation (Weinaug and Katz, 1943)) and those derived from a thermodynamic approach (*e.g.*, the Shereshefsky model (Shereshefsky, 1967), the Connors–Wright (CW) model (Connors and Wright, 1989), the Fu et al. model (Jufu et al., 1986), and the Chunxi et al. model (Chunxi et al., 2000, which is also referred to in the literature as the Li et al. model)). More computationally intensive models of mixture surface tension employ principles of statistical mechanics, and this group of approaches includes density gradient theory (Breure and Peters, 2012; Cornelisse et al., 1993; Cumicheo et al., 2018; Enders and Kahl, 2008; Garrido and Polishuk, 2018; Liang et al., 2016; Lin et al., 2008; Miqueu et al., 2004; Niño Amézquita et al., 2010; Pereira et al., 2016; Sahimi and Taylor, 1991; Zhu et al., 2014), linear gradient theory (Liang et al., 2016; Pereira et al., 2016; Zuo and Stenby, 1998), density functional theory (Klink et al., 2015; Li and Firoozabadi, 2009; Llovell et al., 2010; Sarman et al., 2000; Talreja et al., 2012), and Monte Carlo or molecular dynamics simulations (Cárdenas and Mejía, 2016; Miqueu et al., 2011; Neyt et al., 2013).

The parachor model for mixtures relates the quartic-root of surface tension to phase compositions, densities, and pure-component parachor values. It has been used extensively in the petroleum industry for predicting the surface tension of hydrocarbon mixtures (Fanchi, 2007; Jin and Firoozabadi, 2016; Pereira et al., 2016; Schechter and Guo, 2007; Sherafati and Jessen, 2017). Although the parachor model may be easy to use, its inconsistent predictive power over a wide range of compositions has been reported (Ali, 1994; Lin et al., 2008; Miqueu et al., 2008; Pereira et al., 2016), and numerous variations have been proposed where the quartic root is modified or the pure-component parachor values are adjusted (Ali, 1994; Escobedo and Mansoori, 1998; Schechter and Guo, 2007) to improve its accuracy.

The thermodynamic models have been used for liquid mixtures where all components are in a subcritical state with respect to their critical temperatures and pressures, including aqueous and nonaqueous solutions. Each of these models—Shereshefsky (1967), Connors and Wright (1989), Jufu et al. (1986), Chunxi et al. (2000)—require semi-empirical parameters that are obtained from fitting to experimental data of surface tension as a function of liquid-phase composition. The Connors and Wright (1989), Jufu et al. (1986), and Chunxi et al. (2000) models have two adjustable parameters in a mathematical form that can accurately capture the trend of surface tension as a function of composition, including for nonideal aqueous mixtures. The Shereshefsky model (Shereshefsky, 1967) uses only one fitting parameter and can be used to accurately predict surface tension for a narrower range of mixtures than the models with more parameters.

For the statistical mechanics models that calculate molecular distributions through the interface, the presence of each additional compound in a mixture expands the system of differential equations, which are usually solved via time-consuming iterations, bringing the required number of calculations to the millions (Larsen et al., 2016). These density-theory models need to be coupled with a series of judiciously-chosen Helmholtz free energy functionals which are dependent on density distributions to predict the interfacial properties. Importantly, the accuracy of surface tension predictions made by the density-theory models depends directly on whether the selected Helmholtz free energy functionals accurately predict the liquid-phase density at each composition of interest (Zhu et al., 2014).

The parachor model and the statistical mechanics approaches are capable of predicting the surface tension of mixtures as a function of both composition and temperature (*vs.*, for example, the Chunxi et al. (2000) and Shereshefsky (1967) composition models that must be fit to experimental data separately at each temperature, because their coefficients vary with temperature (Shardt and Elliott, 2017)). However, the accuracy of the parachor model for temperature-dependence is limited by its deficiencies for capturing composition-dependence. The primary drawbacks of the statistical mechanics models are their computational complexity and dependence on the Helmholtz free energy approximations whose accuracy must span wide ranges of temperature and pressure (often, temperature-dependent parameters are used). Thus, there remains a gap in the literature for an easy-to-use, accurate model that reliably describes the surface tension of a broad range of mixtures as a function of both composition and temperature with parameters that can be assumed composition and temperature independent.

In our previous work (Shardt and Elliott, 2017), we proposed an extension of the Connors–Wright model for predicting the surface tension of binary aqueous mixtures (σ_{mix}; N/m) as a function of liquid-phase composition and temperature, and the equation had the following form:

$$\sigma_{\text{mix}}(x_1, T) = \sigma_2(T) - \left(1 + \frac{b(1-x_1)}{1-a(1-x_1)}\right) x_1(\sigma_2(T) - \sigma_1(T)), \qquad (1)$$

where x_1 is the liquid mole fraction of the nonaqueous compound varying between 0 and 1 (that is, both components are below their pure species critical points), T is the absolute temperature, σ_2 is the surface tension of water, and σ_1 is the surface tension of the nonaqueous compound. The unitless coefficients a and b were obtained by fitting to surface tension data as a function of composition at a reference temperature (any temperature for which there is a sufficient number of experimental data points to adequately capture the trend in surface tension) and then used predictively at other temperatures (the coefficients a and b were demonstrated to be temperature independent (Shardt and Elliott, 2017)). To make predictions of surface tension, our method needs accurate experimental data as inputs, including: (*i*) each pure component's surface tension as a function of temperature, and (*ii*) the mixture's surface tension as a function of composition at one temperature.

To briefly summarize the results of our previous work (Shardt and Elliott, 2017), when we tested predictions from Eq. (1) against experimental surface tension data for 15 aqueous mixtures, we obtained an average relative deviation from experimental measurements of 0.62% (where the relative deviation is given by $|\hat{\sigma}_i - \sigma_i|/\sigma_i$ given $\hat{\sigma}_i$ is the prediction and σ_i is the measurement) over all available temperatures (a minimum temperature of 293 K or 298 K with a maximum temperature of 323 K for all systems except for one that spanned 303 K to 373 K) (Shardt and Elliott, 2017). Importantly, we used Eq. (1) to make predictions of surface tension for nitrogen(1) + argon(2) mixtures at tempera-

tures for which experimental data are lacking (Shardt and Elliott, 2018); this equation enabled us to accurately predict the experimentally-determined vapor–liquid equilibrium behavior (dew temperatures) of this mixture in nanopores (Alam et al., 2000). (See the Supplementary Material, Section S8 for a more detailed discussion on the importance of surface tension in these predictions.).

In this work, we further extend Eq. (1) to apply to nonaqueous systems that may contain a supercritical component by introducing a reduced mole fraction. Empirical parameters are assumed constant (independent of temperature) so that predictions can be made at temperatures other than the one used for determining the fitting coefficients. In addition to the two inputs listed for Eq. (1), we need one additional input: (*iii*) the critical composition of the binary mixture obtained from an equation of state. For this input, we develop a numerical method to calculate the value of the critical composition at a given temperature. An important benefit of our approach is that the molar volumes of the liquid and vapor phases are not needed for surface tension predictions, whereas the parachor model and the statistical mechanics models (density gradient theory and density functional theory) all require accurate values for the molar volumes over all compositions and temperatures of interest.

If experimentally measured surface tensions as a function of composition at even a single temperature are unavailable for a specific mixture of interest, a statistical mechanics model could instead be used to obtain these values, which could be used as an input to our model for predictions at any composition and temperature. In this way, a hybrid approach that uses our equation together with inputs from a statistical mechanics model would reduce the overall computational cost required to calculate surface tension as a function of all compositions and temperatures.

We note that throughout this paper, the use of "supercritical" to describe a mixture does not indicate that it is in a state above the critical point of the mixture; rather, we use this term to denote that one of the components is in a supercritical state with respect to its pure-component critical point, while the mixture is still within the two-phase vapor–liquid phase envelope. The use of "subcritical" refers to a mixture where each pure component is below its individual critical point.

2. Governing equations and numerical methods

Based on Eq. (1), we propose the following equation for the surface tension of a binary mixture as a function of liquid mole fraction and temperature:

$$\sigma_{\text{mix}}(x_{1,\text{r}},T)=\sigma_2(T)-\left(1+\frac{b(1-x_{1,\text{r}}(T))}{1-a(1-x_{1,\text{r}}(T))}\right)x_{1,\text{r}}(T)(\sigma_2(T)-\sigma_1(T)), \tag{2}$$

where σ_{mix} is the surface tension of the mixture at an absolute temperature T, σ_i is the surface tension of pure component i (where $\sigma_2>\sigma_1$), the reduced mole fraction of component 1 is $x_{1,\text{r}}(T)=x_1/x_{1,\text{cr}}(T)$ where $x_{1,\text{cr}}$ is the critical composition of component 1 at the given temperature (*i.e.*, the maximum liquid-phase composition on the isothermal phase diagram of the binary mixture). Although there are numerous approaches in the literature for calculating the critical temperature and pressure of a multicomponent system given its composition (Firoozabadi, 2016; Peng and Robinson, 1977; Heidemann and Khalil, 1980; Michelsen, 1984; Stradi et al., 2001), the reverse calculation—determining the critical composition at a given temperature—is less studied and more challenging. We develop a numerical method for calculating the critical composition of a mixture, and in implementing this method, we choose the Peng–Robinson equation of state (PR-EOS) (Peng and Robinson, 1976; Robinson and Peng, 1978). Briefly, our numerical approach is to trace the outline of the vapor–liquid phase envelope until convergence at the critical composition is achieved (see the Supplementary Material, Section S2 for further details on our iterative numerical method, which could be adapted for mixtures of interest outside of those studied herein). In contrast to the intensity of calculations for density gradient theory models that require discretizing a system of differential equations coupled to an equation of state, the calculation of the critical composition needs only the equation of state. In this respect, the critical composition could be considered a more accessible quantity, although the termination criterion in our outlined iterative solution approach may require fine-tuning for a specific mixture of interest. Additionally, the computational cost of our approach is lower over the variable space of composition and temperature, because the calculation of the critical composition only needs to be done at each temperature of interest and it can then be used for any mixture composition at that temperature. In contrast, the equations that govern density gradient theory need to be solved whenever either composition or temperature changes. The values of a and b are specific to each binary mixture, and they are determined by fitting to experimental data as a function of mole fraction at one temperature. Note that when $T>T_{\text{cr},1}$ (or equivalently, $x_{1,\text{cr}}<1$), $\sigma_1=0$. Eq. (2) can also be used for subcritical mixtures in the limiting case where $x_{1,\text{cr}}=1$, in which case the equation reduces to Eq. (1).

To apply our approach beyond binary mixtures, we develop a multicomponent form of Eq. (2). To do so, we start with the multicomponent equation for surface tension proposed by Chunxi et al. (2000) and convert the proposed coefficients to those proposed by Connors and Wright (1989) (see Shardt and Elliott, (2017) for equations to convert between the Chunxi et al. and CW models). Then, we introduce a reduced mole fraction for each component of the multicomponent mixture to yield the following equation:

$$\sigma_{\text{mix}}(x_{i,\text{r}},T)=\sum_{i=1}^{n}\sigma_i(T)x_{i,\text{r}}(T)+\sum_{i=1}^{n}\frac{x_{i,\text{r}}(T)}{\sum_{j=1}^{n}\frac{x_{j,\text{r}}(T)}{1-a_{ji}}}\sum_{j=1}^{n}\frac{b_{ji}}{a_{ji}}\left(\frac{1}{1-a_{ji}}\right)(\sigma_i(T)-\sigma_j(T))x_{j,\text{r}}\ (T), \tag{3}$$

where the reduced mole fractions for all components $i>1$ are $x_{i>1,\text{r}}=\frac{x_i}{\sum_{j=2}^{n}x_j}(1-x_{1,\text{r}})$, n is the number of components, and a_{ji} and b_{ji} are fitting coefficients obtained from fitting to surface tension data of a binary mixture made up of components j and i where $\sigma_j>\sigma_i$ at a single temperature for each mixture. Note that when $T>T_{\text{cr},i}$ for any component i, $\sigma_i(T)=0$. Importantly for multicomponent mixtures, the reduced mole fractions are obtained relative to the critical composition of compound 1, which is the first compound to become supercritical. The critical composition in Eq. (3) may be different in value from the critical compositions that were obtained for each binary combination of compounds. In fact, when calculating the critical composition of compound 1 in a mixture with more than two components, the number of degrees of freedom increases, and thus an additional constraint must be specified: the relative proportion of each compound $i>1$ that comprises the mixture. Therefore, to solve for the critical composition of compound 1, we determine the phase envelope of a pseudobinary mixture with overall mixture composition z_1, where the remaining compounds are a fixed fraction of the remaining mole fraction $1-z_1$. A practical example of the solution procedure is outlined in the Supplementary Material, Section S7. Note that the following relationships apply to the coefficients in Eq. (3) when $i=j$:

$$a_{ii} = 0 \tag{4a}$$
$$b_{ii} = 0 \tag{4b}$$
$$\frac{a_{ii}}{b_{ii}} = 1 \tag{4c}$$

and the following apply when $i \neq j$:

$$b_{ij} = b_{ji} \tag{5a}$$
$$(1 - a_{ij}) = (1 - a_{ji})^{-1}. \tag{5b}$$

While Eqs. (2) and (3) show the dependence of surface tension on liquid mole fraction, the surface tension of supercritical mixtures is instead commonly reported in the experimental literature as a function of pressure at a given temperature. Pressure only affects the surface tension of the supercritical mixtures in an indirect way, as it directly changes the liquid-phase composition through a shift in the equilibrium state of the vapor–liquid system; it is because of this change in composition that the surface tension changes. To obtain the composition-dependence of experimental surface tension in the literature, we use the PR-EOS with appropriate binary interaction parameters to calculate the liquid-phase compositions of supercritical binary mixtures at the reported temperatures and pressures. (See the Supplementary Material, Section S1 for all governing equations and validation of our calculations against experimental vapor–liquid equilibrium data from the literature.)

Matlab R2018a (Natick, MA, USA) was used for all fitting procedures and calculations. Refer to the Supplementary Material, Sections S1–S4 for more detailed fitting and calculation methods.

3. Results

3.1. Temperature dependence of pure component surface tensions

First, we calculate pure component surface tensions at the temperature of interest where we use either: (*i*) the Mulero et al. correlation (Mulero et al., 2012) for the supercritical mixtures (those containing methane or carbon dioxide):

$$\sigma_i = \sum_{j=0}^{m_i} \sigma_{j,i} \left(1 - \frac{T}{T_{\mathrm{cr},i}}\right)^{p_{j,i}}, \tag{6}$$

where $T_{\mathrm{cr},i}$ is the critical temperature (K) and the values of $\sigma_{j,i}$, $p_{j,i}$ and m_i are specific to each compound (see the Supplementary Material, Table S4); or (*ii*) a linear equation

$$\sigma_i = \theta_{0,i} + \theta_{1,i} T \tag{7}$$

Table 1
For mixtures with both components below their critical point, fitting coefficients with 95% confidence intervals (CI) are listed for each pure component for T in K and σ_i in mN/m with a linear fit ($\sigma_i = \theta_{0,i} + \theta_{1,i}T$) to n experimental data points from each reference. Note, for some datasets, all experimental data lies exactly on the linear fit, the standard deviation (SD) is zero, and the confidence interval cannot be calculated.

Component	n	Temperatures [K]	$\theta_{0,i} \pm 95$ % CI	$\theta_{1,i} \pm 95$ % CI	SD [mN/m]	Data Reference
Dodecane(1)	4	298–313	50.23 ± 3.09	-0.086 ± 0.010	0.026	Schmidt et al. (1966)
Benzene(2)	4		68.10	−0.134	0	
n-Hexane(1)	4	298–313	49.01 ± 0.70	-0.104 ± 0.002	0.006	Schmidt et al. (1966)
Benzene(2)	4		68.10	−0.134	0	
Cyclohexane(1)	4	293–313	57.35 ± 11.70	-0.111 ± 0.039	0.133	Herrmann (1994, 1997)
Benzene(2)	4		64.85 ± 4.90	-0.123 ± 4.898	0.056	
Carbon tetrachloride(1)	5	288–308	66.26	−0.134	0	Teixeira et al. (1992)
Methyl iodide(2)	5		67.13 ± 0.19	-0.123 ± 0.190	0.003	
Carbon tetrachloride(1)	5	298–318	66.26	−0.134	0	Teixeira et al. (1992)
Acetonitrile(2)	5		66.41 ± 0.20	-0.127 ± 0.196	0.003	
Carbon tetrachloride(1)	6	293–318	62.92 ± 0.18	-0.122 ± 0.001	0.004	Luengo et al. (1988)
Carbon disulfide(2)	6		73.48 ± 1.42	-0.140 ± 1.418	0.035	
Dichloromethane(1)	4	293–308	65.54 ± 0.45	-0.129 ± 0.002	0.004	Aracil et al. (1989)
Carbon disulfide(2)	4		75.71	−0.148	0	

Table 2
Fitting coefficients (a and b) with 95% confidence intervals for Eq. (2) for binary organic systems with corresponding fitting temperature (T_{fit}), critical composition of component 1 ($x_{\mathrm{cr},1}$), number of points used (n), and standard deviation of the fit (SD). The literature source for experimental data is listed under the heading "Data Reference".

Component 1	Component 2	n	T_{fit} [K]	$x_{\mathrm{cr},1}(T_{\mathrm{fit}})$	$a \pm 95$ % CI	$b \pm 95$ % CI	SD [mN/m]	Data Reference
Methane	Ethane	6	133	1.000	0.52 ± 0.89	0.50 ± 0.44	0.49	Baidakov et al. (2013)
	Propane	6	258	0.776	-1.42 ± 0.81	1.53 ± 0.34	0.07	Weinaug and Katz (1943)
	n-Butane	6	311	0.730	-2.43 ± 0.54	2.06 ± 0.22	0.01	Nilssen (2008, 1965)
	n-Hexane	8	298	0.846	-1.49 ± 0.77	2.08 ± 0.55	0.05	Massoudi and King (1975)
	n-Heptane	16	311	0.860	-1.44 ± 0.26	1.53 ± 0.09	0.11	Amin and Smith (1998)
	n-Decane	23	311	0.902	-2.01 ± 0.21	1.49 ± 0.05	0.09	Stegemeier et al. (1962)
Carbon dioxide	*n*-Butane	18	319	0.871	0.70 ± 0.13	0.41 ± 0.06	0.12	Hsu et al. (1985)
	n-Heptane	6	323	0.957	-1.91 ± 2.69	0.91 ± 0.59	0.21	Niño Amézquita et al. (2010)
Dodecane	Benzene	5	298	1.000	0.86 ± 0.07	1.06 ± 0.13	0.04	Schmidt et al. (1966)
n-Hexane	Benzene	7	298	1.000	0.80 ± 0.04	0.51 ± 0.03	0.05	Schmidt et al. (1966)
Cyclohexane	Benzene	11	293	1.000	0.43 ± 0.20	0.84 ± 0.13	0.07	Herrmann (1994), Wohlfarth and Wohlfarth (1997)
Carbon tetrachloride	Methyl iodide	5	288	1.000	0.66 ± 0.08	1.00 ± 0.10	0.03	Teixeira et al. (1992)
	Acetonitrile	9	298	1.000	0.82 ± 0.06	0.69 ± 0.07	0.03	Teixeira et al. (1992)
	Carbon disulfide	10	293	1.000	0.56 ± 0.18	0.77 ± 0.15	0.11	Luengo et al. (1988)
Dichloromethane	Carbon disulfide	8	293	1.000	0.45 ± 0.22	1.05 ± 0.20	0.09	Aracil et al. (1989)

fit to the reported data for each pure component comprising the subcritical mixtures (all coefficients used are summarized in Table 1).

3.2. Fitting parameters at a reference temperature

Our next set of results is the fitting coefficients for the composition dependence of surface tension at a single temperature for a range of supercritical and subcritical mixtures available in the literature. Substituting the values of each pure component's surface tension obtained via Eqs. (6) or (7) into Eq. (2), we fit Eq. (2) to experimental data of surface tension as a function of composition at a single temperature with critical composition $x_{cr,1}$ to obtain the coefficients a and b listed in Table 2. Given that the fit of surface tension *vs.* liquid mole fraction is a nonlinear equation (Eq. (2)), the goodness of fit is indicated by the standard deviation (SD), which is calculated by $SD = \sqrt{\frac{\sum(\hat{\sigma}_i - \sigma_i)^2}{n-p}}$, where n is the number of points used in the fit, $p = 2$ is the number of fitting coefficients, $\hat{\sigma}_i$ is predicted surface tension, and σ_i is experimental surface tension. A list of systems available in the literature is included in the Supplementary Material, Section S5 with detailed notes on the reliability and suitability of data for fitting (briefly, some datasets are in disagreement with other literature sources and others report insufficient data points for fitting purposes).

Table 3
Our calculated critical composition of methane as a function of the temperatures listed in each literature source for methane(1) + *n*-alkane(2) mixtures.

Methane(1) +	Temperature [K]	Critical Composition $x_{1,cr}$	Data Reference
Ethane(2)	133.15	1.000	Baidakov et al. (2013)
	173.15	1.000	
	193.15	0.985	
	213.15	0.869	
	233.15	0.737	
	253.15	0.589	
	263.15	0.505	
	273.15	0.412	
	283.15	0.305	
Propane(2)	258.15	0.776	Weinaug and Katz (1943)
	283.15	0.685	
	303.15	0.596	
	318.15	0.513	
	338.15	0.370	
	272.20	0.727	Seneviratne et al. (2017)
	285.50	0.675	
	303.34	0.595	
n-Butane(2)	310.93	0.730	Nilssen (2008, 1965)
	327.59	0.685	
	335.93	0.660	
	344.26	0.631	
n-Hexane(2)	298.15	0.846	Massoudi and King (1975)
	300.00	0.845	Niño Amézquita et al. (2010)
	350.00	0.796	
n-Heptane(2)	310.93	0.860	Warren and Hough (1970)
	327.59	0.850	
	344.26	0.838	
	360.93	0.823	
	377.59	0.806	
	394.26	0.787	
	410.93	0.763	
	427.59	0.734	
	310.93	0.860	Amin and Smith (1998)
	338.71	0.842	
	366.48	0.818	
	394.26	0.787	
n-Decane(2)	310.93	0.902	Stegemeier et al. (1962)
	327.59	0.898	
	344.26	0.893	
	360.93	0.887	
	310.93	0.902	Amin and Smith (1998)
	366.48	0.884	
	410.93	0.862	
	313.30	0.901	Pereira et al. (2016)
	343.20	0.893	
	392.60	0.873	
	442.30	0.841	

3.3. Predictions of surface tension

Having obtained fitting coefficients at one temperature, we assume that these coefficients (a and b) are temperature-independent, and we make predictions of surface tension as a function of liquid-phase composition using Eq. (2) for all elevated temperatures studied experimentally. At each considered temperature, the critical composition is calculated, with values summarized in Tables 3 and 4. For the pure-component surface tensions in Eq. (2), we use the Mulero et al. correlation (Eq. (6)) (Mulero et al., 2012) for pure components comprising supercritical mixtures or the linear equation (Eq. (7)) for those comprising subcritical mixtures.

We make predictions of surface tension for six methane(1) + *n*-alkane(2) systems and two carbon dioxide(1) + *n*-alkane(2) systems for a total of 466 experimental points over a wide range of temperatures (173–442 K) and pressures (0.1–35.9 MPa), obtaining an average absolute difference between experiments and predictions of 0.22 mN/m over all systems. In addition, we use our equation for seven subcritical mixtures (236 data points, e.g., Lam and Benson, 1970; Konobeev and Lyapin, 1970), obtaining predictions that are an average absolute difference of 0.09 mN/m away from experimental measurements. For the ternary mixture methanol(1) + ethanol(2) + water(3), surface tension predictions using Eq. (3) are an average absolute deviation of 0.71 mN/m away from 196 experimental measurements at various concentrations (both dilute and concentrated) and at temperatures between 278 K and 333 K. Because our equation is computationally simple, it can be easily implemented in any application of interest and in any process simulation software for liquid mixtures. Significantly, our equation achieves an accuracy that is comparable to that achieved by the density gradient and density functional theories (reported average absolute deviations obtained with these theories include: 0.05 mN/m for carbon dioxide(1) + *n*-decane(2) at 344.3 K (Klink et al., 2015); 0.23 mN/m for a variety of binary hydrocarbon mixtures (403 data points for T between 278.28 K and 442.55 K) (Zhu et al., 2014); and 0.23 mN/m for a variety of binary halogenated hydrocarbon mixtures (885 points for T between 223.15 K and 343.16 K) (Lin et al., 2008).

For comparison, we also make surface tension predictions using the parachor model (Weinaug and Katz, 1943) with volume-shifted PR-EOS phase densities of the mixture (Ahlers and Gmehling, 2001) and pure-component parachor values obtained from fitting

Table 4
Our calculated critical composition of carbon dioxide as a function of temperature for carbon dioxide(1) + *n*-alkane(2) mixtures.

Carbon dioxide(1) +	Temperature [K]	Critical Composition $x_{1,cr}$	Data Reference
n-Butane(2)	319.30	0.871	Hsu et al. (1985)
	344.30	0.725	
	377.60	0.517	
n-Heptane(2)	323.15	0.957	Niño Amézquita et al. (2010)
	353.15	0.885	
	323.00	0.958	Jaeger et al. (2010)
	353.00	0.885	

pure-component PR-EOS phase densities (also volume-shifted) to temperature-dependent surface tension data retrieved from the DIPPR database ((Design Institute for Physical Properties, 2019); see the Supplementary Material, Section S4). We compile the performance of our new model and the parachor model in Table 5 with a list of the average absolute deviation $\left(\text{AAD} = \frac{1}{j}\sum_{i=1}^{j}|\hat{\sigma}_i - \sigma_i|\right)$ and maximum absolute deviation for each studied mixture. Over the broad range of supercritical hydrocarbon mixtures and subcritical organic mixtures, our new model has an AAD of 0.18 mN/m compared to the parachor model's AAD of 0.48 mN/m. We also calculate the average $\left(\frac{1}{j}\sum_{i=1}^{j}\frac{|\hat{\sigma}_i-\sigma_i|}{\sigma_i}\right)$ and maximum percent relative deviation for each system (Table 6) for all points where the experimental surface tension $\sigma_i \geqslant 0.1$ mN/m (this cutoff was chosen because relative deviations lose meaning as surface tension approaches zero; additionally, whether equilibrium has been reached in the critical region can be difficult to determine when making experimental measurements). Our new model has an average relative deviation of 7.1% over all studied systems compared to the parachor model's 14.1% average relative deviation.

As representative systems of the supercritical set of studied mixtures, we show detailed results for methane(1) + ethane(2) and carbon dioxide(1) + *n*-butane(2) in Fig. 1, where the dashed black lines show the fit of Eq. (2) to experimental data (black circles) at the lowest available temperature. All solid lines are predictions using Eq. (2) at elevated temperatures with critical compositions calculated from the PR-EOS and with pure-component surface tensions evaluated using Eq. (6) (coefficients in the Supplementary Material, Table S4); these predictions closely

Table 5
Average absolute deviations from experimental data $\left(\frac{1}{j}\sum_{i=1}^{j}|\hat{\sigma}_i - \sigma_i|\right)$ and maximum absolute deviations $(|\hat{\sigma}_i - \sigma_i|)$ of surface tension predictions obtained using either our new model (Eq. (2)) or the parachor model (see the Supplementary Material, Section S5) for each considered binary mixture over a range of temperatures and pressures with j points from each listed literature source. The last row considers all studied systems. The columns for average absolute deviation are shaded with a color gradient from dark blue (0 mN/m) to white (0.6 mN/m) to dark red (1.2 mN/m). White text on a blue background indicates that the value is less than 0.2 mN/m.

					Parachor model absolute deviation [mN/m]		New model absolute deviation [mN/m]		
Component 1	Component 2	Temperatures [K]	Pressures [MPa]	j	Average	Max	Average	Max	Data Reference
methane	ethane	173–283	0.1–3.9	58	0.56	1.26	0.16	0.45	Baidakov et al. (2013)
	propane	283–338	1.4–8.5	36	0.33	0.48	0.17	0.27	Weinaug and Katz (1943)
		272–303	1.0–8.7	24	0.26	0.32	0.22	0.26	Seneviratne et al. (2017)
	n-butane	328–344	9–10	9	0.23	0.32	0.08	0.11	Nilssen (2008), Pennington and Hough (1965)
	n-hexane	300–350	2–10	9	0.26	0.36	0.34	0.49	Niño Amézquita et al. (2010b)
	n-heptane	311–428	2.8–24.8	101	0.44	0.62	0.16	0.24	Warren and Hough (1970)
		339–394	2.8–24.1	37	0.28	0.41	0.08	0.13	Amin and Smith (1998)
	n-decane	328–361	10.3–35.9	52	0.27	0.51	0.06	0.12	Stegemeier et al. (1962)
		311–411	2.8–34.5	55	1.24	1.58	0.46	0.76	Amin and Smith (1998)
		313–442	0.5–30.5	39	0.69	0.89	0.59	0.82	Pereira et al. (2016)
carbon dioxide	*n*-butane	344–378	2.9–8.0	24	0.26	0.40	0.12	0.21	Hsu et al. (1985)
	n-heptane	353	0.1–11.2	8	0.21	0.42	0.15	0.29	Niño Amézquita et al. (2010a)
		323–353	0.1–11.2	14	0.53	0.55	0.26	0.29	Jaeger et al. (2010)
dodecane	benzene	303–313	–	12	0.27	0.40	0.10	0.20	Schmidt et al. (1966)
n-hexane	benzene	303–313	–	10	0.61	0.87	0.14	0.22	Schmidt et al. (1966)
cyclohexane	benzene	293–303	–	28	0.43	0.44	0.09	0.13	Lam and Benson (1970)
		293–333	–	33	0.66	0.94	0.10	0.18	Konobeev and Lyapin (1970), Wohlfarth (1997)
		298–313	–	27	0.37	0.55	0.08	0.14	Herrmann (1994), Wohlfarth (1997)
carbon tetrachloride	methyl iodide	293–308	–	34	0.47	0.61	0.05	0.09	Teixeira et al. (1992)
	acetonitrile	303–318	–	29	0.42	0.56	0.04	0.08	Teixeira et al. (1992)
	carbon disulfide	298–318	–	40	0.14	0.31	0.10	0.19	Luengo et al. (1988)
dichloromethane	carbon disulfide	298–308	–	23	0.83	1.15	0.18	0.29	Aracil et al. (1989)
all systems		173–442		702	0.48	1.58	0.18	0.82	

Table 6
Average relative deviations from experimental data $\left(\frac{1}{j}\sum_{i=1}^{j}\frac{|\hat{\sigma}_i-\sigma_i|}{\sigma_i}\right)$ and maximum relative deviations $\left(\frac{|\hat{\sigma}_i-\sigma_i|}{\sigma_i}\right)$ of surface tension predictions obtained using either our new model (Eq. (2)) or the parachor model (see the Supplementary Material, Section S5) for each considered binary mixture over a range of temperatures and pressures with j points from each listed literature source that satisfy $\sigma_i \geqslant 0.1$ mN/m. The last row considers all studied systems. The columns for average relative deviation are shaded with a color gradient from dark blue (0%) to white (20%) to dark red (40%). White text on a blue background indicates that the average deviation is less than 5%.

			Parachor model relative deviation [%]		New model relative deviation [%]		
Component 1	Component 2	j where $\sigma_i \geq 0.1$ mN/m	Average	Max	Average	Max	Data Reference
methane	ethane	58	16.1	43.5	3.8	8.4	Baidakov et al. (2013)
	propane	36	21.4	48.3	11.7	18.4	Weinaug and Katz (1943)
		24	13.0	19.7	14.2	28.3	Seneviratne et al. (2017)
	n-butane	9	21.3	33.5	7.3	10.2	Nilssen (2008), Pennington and Hough (1965)
	n-hexane	9	4.7	6.5	5.3	6.2	Niño Amézquita et al. (2010b)
	n-heptane	93	23.4	33.9	10.8	19.8	Warren and Hough (1970)
		36	16.0	24.5	6.9	13.1	Amin and Smith (1988)
	n-decane	40	20.8	33.2	11.1	17.5	Stegemeier et al. (1962)
		54	28.5	35.3	7.4	10.1	Amin and Smith (1998)
		39	17.8	22.9	10.9	13.8	Pereira et al. (2016)
carbon dioxide	*n*-butane	19	35.6	57.7	32.7	49.5	Hsu et al. (1985)
	n-heptane	8	5.1	10.3	18.9	37.9	Niño Amézquita et al. (2010a)
		14	22.3	26.7	20.2	22.8	Jaeger et al. (2010)
dodecane	benzene	12	1.1	1.5	0.4	0.8	Schmidt et al. (1966)
n-hexane	benzene	10	2.9	4.1	0.7	1.0	Schmidt et al. (1966)
cyclohexane	benzene	28	1.7	1.8	0.4	0.5	Lam and Benson (1970)
		33	2.9	4.4	0.4	0.7	Konobeev and Lyapin (1970), Wohlfarth (1997)
		27	1.5	2.3	0.3	0.6	Herrmann (1994), Wohlfarth (1997)
carbon tetrachloride	methyl iodide	34	1.8	2.3	0.2	0.4	Teixeira et al. (1992)
	acetonitrile	29	1.7	2.2	0.2	0.3	Teixeira et al. (1992)
	carbon disulfide	40	0.6	1.2	0.4	0.8	Luengo et al. (1988)
dichloromethane	carbon disulfide	23	3.1	4.2	0.7	1.1	Aracil et al. (1989)
all systems		675	14.1	57.7	7.1	49.5	

agree with experimental trends of surface tension. Dotted lines are predictions calculated using the parachor model for mixtures ((Weinaug and Katz, 1943); the Supplementary Material, Eq. (S.22)), which performs with mixed accuracy.

Fig. 2 shows detailed results for two representative systems from the group of studied subcritical organic mixtures: dodecane (1) + benzene(2) and dichloromethane(1) + carbon disulfide(2). The fit of Eq. (2) to experimental data of surface tension is shown at the lowest temperature (dashed black line), along with predictions using Eq. (2) at all elevated temperatures (see Table 1 for the linear equation used for each pure component's surface tension *vs.* temperature). The parachor model predictions are shown with dotted lines. Our model predictions consistently outperform the parachor model over the available range of experimental temperatures and compositions.

Fig. 3 graphically summarizes the accuracy of predictions for all binary systems to which we have applied our model: methane(1) + *n*-alkane(2), carbon dioxide(1) + *n*-alkane(2), various subcritical organic mixtures, and aqueous mixtures. Fitting coefficients to describe the composition-dependence of surface tension for all nonaqueous systems are listed in Table 2, and the temperature-dependence of each pure component is obtained using the Mulero et al. correlation (Eq. (6)) (Mulero et al., 2012) or the linear equation (Eq. (7)) using the coefficients in Table 1. For the coefficients obtained for aqueous systems, refer to Shardt and Elliott, (2017). All points used for fitting purposes are excluded from this figure (any at T_{fit} listed in Table 2 and any pure component values).

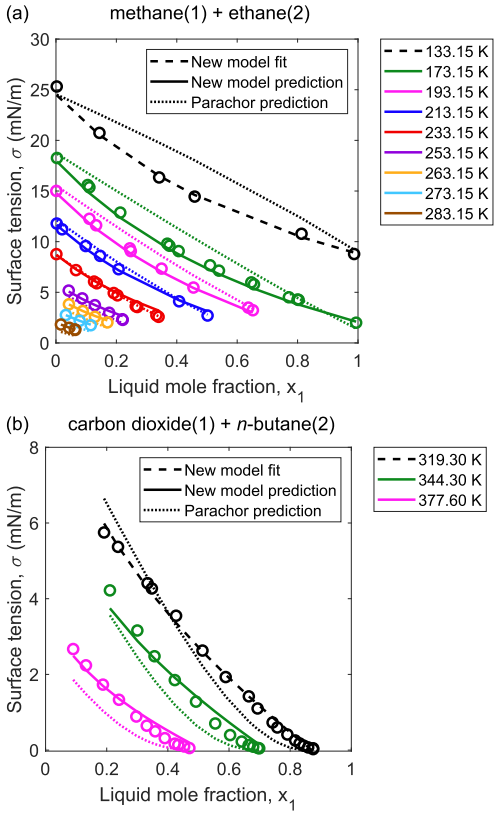

Fig. 1. Fits (dashed black lines using Eq. (2)) and predictions of surface tension (solid lines using Eq. (2); dotted lines using the parachor model (the Supplementary Material, Eq. (S.22)) as a function of liquid-phase composition for (a) methane(1) + ethane(2) and (b) carbon dioxide(1) + *n*-butane(2). Experimental data points (○) that are used in fits are shown in black; all other symbol colors serve as comparisons to theoretical predictions in the same color at the listed temperatures. Data in (a) are from Baidakov et al. (2013) and in (b) are from Hsu et al. (1985). (For interpretation of the references to colour in this figure caption, and the colours in the figure legends themselves, the reader is referred to the web version of this article.).

Fig. 3 highlights that our model accurately predicts the surface tension of a wide variety of nonideal mixtures (nonideal in the sense that $\sigma_{\text{mix}} \neq \sigma_1 x_1 + \sigma_2 x_2$) over a range of temperatures and pressures, and this accuracy is of the same order of magnitude as predictions obtained using density gradient theory or density functional theory (Klink et al., 2015; Lin et al., 2008; Zhu et al., 2014). Such close agreement is the result of fitting coefficients that can be assumed to be independent of temperature. As shown in Fig. 3, our proposed model can be used for aqueous mixtures in addition to hydrocarbon and organic mixtures, a further benefit over the parachor model that cannot be used for predicting the surface tension of aqueous mixtures. As previously noted by Li and Firoozabadi (2009, 2016) and Pereira et al. (2016), we likewise note the unexpectedly high surface tension measurements at low pressures for methane(1) + *n*-decane(2) from Amin and Smith (1998) that are within the dashed oval in Fig. 3. For details of each individual system in Table 3, refer to the Supplementary Material, Section S5 for plots of vapor–liquid equilibrium, critical composition, surface tension as a function of composition (and pressure for supercritical systems), and the difference between predictions and experimental data.

Finally, we make predictions for the surface tension of the ternary mixture methanol(1) + ethanol(2) + water(3) as a function of composition and temperature using Eq. (3), as illustrated in Fig. 4. The inputs to these predictions are (*i*) coefficients to describe surface tension as a function of temperature for each pure compo-

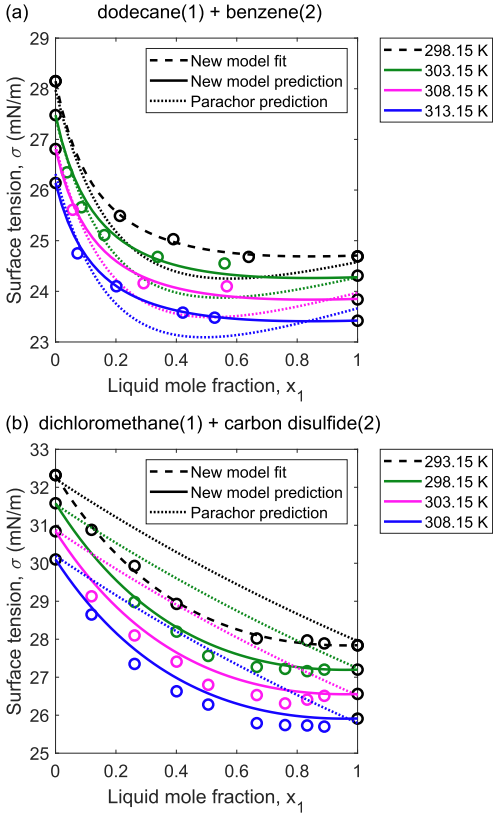

Fig. 2. Fits (dashed black lines using Eq. (2)) and predictions of surface tension (solid lines using Eq. (2); dotted lines using the parachor model (the Supplementary Material, Eq. (S.22)) as a function of liquid-phase composition for (a) dodecane(1) + benzene(2) and (b) dichloromethane(1) + carbon disulfide(2). Experimental data points are shown by open circles (○; black symbols are used in fits: both pure components *vs.* temperature and mixture data at one temperature; all other symbol colors serve as comparisons to theoretical predictions in the same color at the listed temperatures). Data in (a) are from Schmidt et al. (1966) and in (b) are from Aracil et al. (1989) (For interpretation of the references to colour in this figure caption, and the colours in the figure legends themselves, the reader is referred to the web version of this article.).

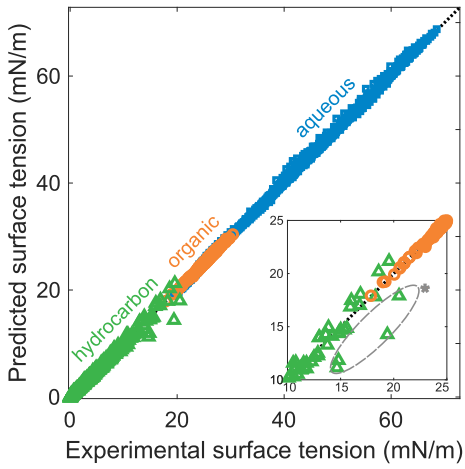

Fig. 3. Predicted surface tension *vs.* experimental surface tension for all methane(1) + *n*-alkane(2) and carbon dioxide(1) + *n*-alkane(2) mixtures (hydrocarbon, △), as well as all binary mixtures where both components are below their pure critical points (organic, ○). We also include all aqueous mixtures (□) from our previous work (Shardt and Elliott, 2017), highlighting the applicability of our approach to a broad range of systems, temperatures, and pressures. This figure contains the 702 points from the 15 supercritical and subcritical systems in Table 5 and 961 points from the 15 aqueous mixtures in Shardt and Elliott (2017). The four points within the dashed circle from the methane(1) + *n*-decane(2) system at low pressures are likely experimental outliers (Amin and Smith, 1998). (For a coloured version of this figure, the reader is referred to the web version of this article.).

nent and (*ii*) coefficients to describe surface tension for each binary mixture as a function of composition at a single temperature (obtained from fitting Eq. (1)). All coefficients used in the predictions illustrated in Fig. 4 are taken from our previous work (Shardt and Elliott, 2017) for binary aqueous systems and are summarized in the Supplementary Material, Tables S14 and S15, and all illustrated experimental data are from Kharin et al. (1968). Surface tension predictions using Eq. (3) are an average absolute deviation of 0.71 mN/m and 2.54% away from experimental measurements of the methanol(1) + ethanol(2) + water(3) mixture for 196 data points at various concentrations (both dilute and concentrated) and at temperatures between 278 K and 333 K. We additionally present ternary predictions for the supercritical ternary mixture carbon dioxide(1) + *n*-butane(2) + *n*-decane(3) in comparison to experimental data obtained by Nagarajan et al. (1990) in the Supplementary Material, Section S7.

4. Discussion

Our new model (Eq. (2)) can be used to predict the surface tension of a wide spectrum of mixtures: those containing supercritical hydrocarbons, subcritical organic compounds, or water. A key benefit of these predictions is that they bypass the calculation of molar volumes for each phase at every temperature, unlike both the parachor model and density gradient theory predictions. This is significant because the estimation of liquid molar volumes in particular

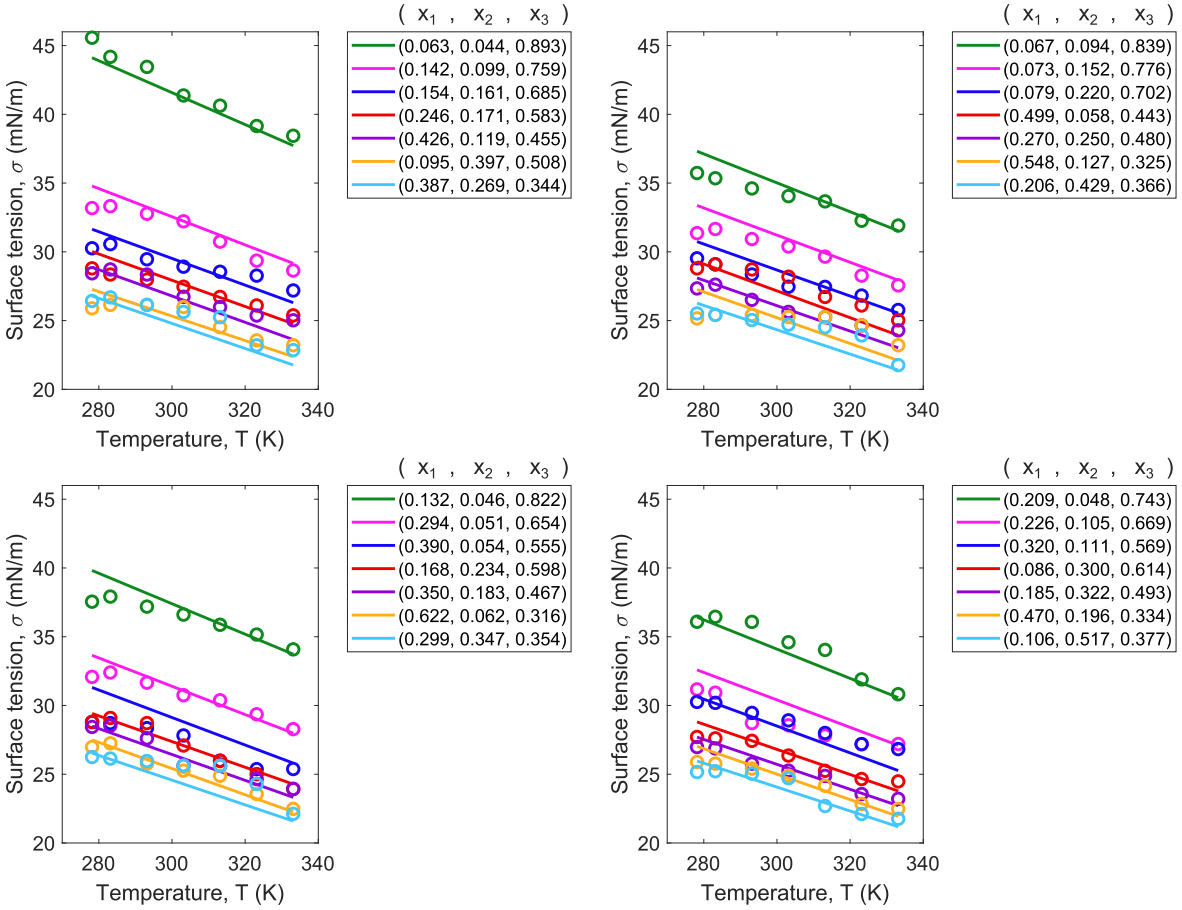

Fig. 4. Surface tension as a function of temperature for mixtures containing methanol(1) + ethanol(2) + water(3), as measured experimentally (symbols) by Kharin et al. (1968) and as predicted by Eq. (3) (lines) with coefficients for each pure component and each aqueous binary mixture at a single temperature from our previous work (Shardt and Elliott, 2017), as summarized in the Supplementary Material, Tables S14 and S15. The mixture compositions (mole fractions of each component computed from the reported weight fractions) are shown in the legend of each graph. No fitting coefficients need to be extracted from surface tension data of the ternary mixture to make predictions. (For interpretation of the colours in the figure legends, the reader is referred to the web version of this article.).

can be a challenge depending on which equation of state is selected (*e.g.*, for the PR-EOS, a volume shift obtained from fitting to experimental data is needed). In contrast to the parachor model and density gradient theory, we constrain our use of the PR-EOS to only determining vapor–liquid phase equilibrium states (compositions of the liquid phase) and the critical compositions of each mixture as a function of temperature. We also demonstrated that our model can be applied to multicomponent mixtures through Eq. (3) for predicting surface tension as a function of composition and temperature. The coefficients used to make these predictions are obtained from each binary mixture that constitutes the ternary one, and these coefficients can be assumed composition- and temperature-independent. No coefficients need to be extracted from the ternary data.

We make two further observations. First, the coefficients a and b in the original Connors–Wright model (Connors and Wright, 1989) upon which we base our work originated from a Langmuir adsorption isotherm that considered the difference in composition between the bulk and the interface for binary aqueous systems. When these coefficients are used for the systems studied herein, however, it appears that this physical link is more tenuous, because the coefficient a varies from being positive to negative among even the same type of mixture (*e.g.*, methane(1) + *n*-alkane(2)), and there is no clear increase or decrease with increasing carbon number as might be expected if a physical link were present. Second, we note that Eq. (2) may predict an unphysical negative surface tension as the critical composition of a supercritical mixture is approached, and we attribute this partly to the empirical nature and functional form of the equation, but also to our use of the PR-EOS in calculating the critical composition of the mixture, which may be different from the true critical composition. Nevertheless, for the wide range of systems, temperatures, and compositions considered, Eq. (2) and its multicomponent form Eq. (3) provide a straightforward approach for accurately predicting surface tension in the diverse applications that are governed by surface effects.

Most importantly, the practical utility of such an equation is in its application to systems for which no experimental data is available. For example, in our previous work (Shardt and Elliott, 2018), we predicted the dew temperatures of a mixture containing nitrogen(1) + argon(2) in nanopores within 0.45% of experimental measurements (Alam et al., 2000); surface tension is the key variable in the system of equations that is used to make these predictions. Since experimental measurements of the surface tension for nitrogen(1) + argon(2) mixtures over a wide range of compositions were available at only a single temperature, we used Eq. (1) to extrapolate to higher temperatures around the dew point of the mixture. If the surface tension is instead assumed to be constant with either temperature or composition, predictions of dew point become increasingly inaccurate (see the Supplementary Material, Section S8).

5. Conclusions

Experimentally, it is feasible to perform surface tension measurements for a pure component at multiple temperatures or for various mixture compositions at a single temperature, but the shear number of experimental measurements required for mixtures over many compositions and temperatures is both time-consuming and costly. Therefore, accurate theoretical predictions of surface tension as a function of both composition and temperature are advantageous for the wide range of mixtures present across various applications and fields of study. The computational simplicity of a theoretical approach is particularly important when surface tension is one piece of a larger system of equations that describe, for example, phase equilibrium (Shardt and Elliott, 2016, 2018).

We present a model of surface tension as a function of composition and temperature applicable to a wide range of supercritical hydrocarbon mixtures, subcritical organic systems, and subcritical aqueous solutions. As a case study, we additionally extend the model to a mixture of cryogenic gases (nitrogen(1) + argon(2)) and investigate the importance of an accurate representation of surface tension for the phase equilibrium of the system in nanopores. Because the coefficients in our model can be assumed composition- and temperature-independent, accurate predictions can be made for conditions where experimental data is unavailable. The development of a simple equation for $\sigma(x_1, T)$ should prove to be useful in understanding, designing, and controlling both natural and industrial processes. For example, concentration and temperature can both be treated as design parameters instead of being limited to either a pure component at any temperature or a mixture at a single temperature.

The only experimental data needed for using our surface tension model for multicomponent systems are: (*i*) surface tension *vs.* temperature for each pure component (*e.g.*, from DIPPR (Design Institute for Physical Properties, 2019)) and (*ii*) surface tension *vs.* composition for each constituent binary mixture of interest at one temperature, which may be found in the literature (*e.g.*, Wohlfarth and Wohlfarth (1997)). Alternatively, if experimental data of surface tension is lacking, predictions obtained from a statistical mechanics model for each binary mixture as a function of composition at one temperature could be used as inputs instead. Our model lowers the overall computational cost required to make predictions of surface tension for each binary mixture at other temperatures and compositions. Additionally, our model can predict the surface tension of mixtures with more than two components *via* Eq. (3) using coefficients obtained from every constituent binary mixture, each at a single temperature (no fitting coefficients need to be extracted from surface tension data of the multicomponent mixture).

If the mixture contains a supercritical compound, the critical composition of this compound needs to be calculated as a function of temperature using an appropriate equation of state. For any of the studied systems, pure-component surface tension *vs.* temperature can be substituted into Eq. (2), the critical composition can be calculated (see the Supplementary Material, Section S2 for a flowchart of our numerical method), and the tabulated coefficients a and b can be used to predict surface tension. Our model is advantageous compared to those in the literature that rely on accurate phase density predictions from equations of state (*e.g.*, the parachor model and density gradient theory predictions), because density predictions are unnecessary as inputs to Eq. (2) or Eq. (3).

Finally, we note a vital need for ensuring the accuracy of experimental measurements for the surface tension of mixtures, particularly those containing supercritical compounds (*e.g.*, methane and carbon dioxide), and a need for a larger database of experimental systems with which predictions can be compared.

CRediT authorship contribution statement

Nadia Shardt: Conceptualization, Methodology, Software, Investigation, Data curation, Validation, Visualization, Formal analysis, Writing - original draft, Writing - review & editing. **Yingnan Wang:** Methodology, Validation, Visualization, Formal analysis, Writing - review & editing. **Zhehui Jin:** Formal analysis, Visualization, Supervision, Resources, Funding acquisition, Writing - review & editing. **Janet A. W. Elliott:** Conceptualization, Formal analysis, Visualization, Supervision, Resources, Funding acquisition, Writing - review & editing.

Declaration of Competing Interest

The authors declare that they have no known competing financial interests or personal relationships that could have appeared to influence the work reported in this paper.

Acknowledgments

We thank Dr. J. M. Shaw for advice on the critical composition of multicomponent mixtures and Dr. A. Komrakova for help in translating Kharin et al. (1968). NS acknowledges funding from the Natural Sciences and Engineering Research Council (NSERC) of Canada, Alberta Innovates and Alberta Advanced Education, the Government of Alberta, and the University of Alberta. JAWE holds a Canada Research Chair in Thermodynamics and acknowledges a Discovery Grant from NSERC (NSERC RGPIN-2016-05502). YW and ZJ also acknowledge a Discovery Grant from NSERC (NSERC RGPIN-2017-05080).

Appendix A. Supplementary material

Supplementary data associated with this article can be found, in the online version, at https://doi.org/10.1016/j.ces.2020.116095.

References

Ahlers, J., Gmehling, J., 2001. Development of an universal group contribution equation of state: I. Prediction of liquid densities for pure compounds with a volume translated Peng-Robinson equation of state. Fluid Phase Equilib. 191, 177–188.
Alam, M.A., Clarke, A.P., Duffy, J.A., 2000. Capillary condensation and desorption of binary mixtures of N_2–Ar confined in a mesoporous medium. Langmuir 16, 7551–7553.
Ali, J.K., 1994. Prediction of parachors of petroleum cuts and pseudocomponents. Fluid Phase Equilib. 95, 383–398.
Amin, R., Smith, T.N., 1998. Interfacial tension and spreading coefficient under reservoir conditions. Fluid Phase Equilib. 142, 231–241.
Aracil, J., Luengo, G., Almeida, B.S., Telo da Gama, M.M., Rubio, R.G., Diaz Pena, M., 1989. Surface properties of mixtures of molecular fluids: an experimental and theoretical study of carbon disulfide + dichloromethane and carbon disulfide + carbon tetrachloride. J. Phys. Chem. 93, 3210–3218.
Arzhavitina, A., Steckel, H., 2010. Surface active drugs significantly alter the drug output rate from medical nebulizers. Int. J. Pharm. 384, 128–136.
Aumann, E., Hildemann, L.M., Tabazadeh, A., 2010. Measuring and modeling the composition and temperature-dependence of surface tension for organic solutions. Atmos. Environ. 44, 329–337.
Baidakov, V.G., Kaverin, A.M., Pankov, A.S., 2012. Nucleation in liquid ethane with small additions of methane. J. Phys. Chem. C 116, 20458–20464.
Baidakov, V.G., Kaverin, A.M., Khotienkova, M.N., 2013. Surface tension of ethane–methane solutions: 1. Experiment and thermodynamic analysis of the results. Fluid Phase Equilib. 356, 90–95.
Bastakoti, D., Zhang, H., Li, D., Cai, W., Li, F., 2018. An overview on the developing trend of pulsating heat pipe and its performance. Appl. Therm. Eng. 141, 305–332.
Blander, M., Hengstenberg, D., Katz, J.L., 1971. Bubble nucleation in n-pentane, n-hexane, n-pentane + hexadecane mixtures, and water. J. Phys. Chem. 75, 3613–3619.
Boyer, H.C., Dutcher, C.S., 2017. Atmospheric aqueous aerosol surface tensions: Isotherm-based modeling and biphasic microfluidic measurements. J. Phys. Chem. A 121, 4733–4742.
Breure, B., Peters, C.J., 2012. Modeling of the surface tension of pure components and mixtures using the density gradient theory combined with a theoretically derived influence parameter correlation. Fluid Phase Equilib. 334, 189–196.
Brock, J.R., Bird, R.B., 1955. Surface tension and the principle of corresponding states. AIChE J. 1, 174–177.
Brown, J.L., 2018. Vapour-Liquid Equilibria within Nanoporous Media Ph.D. thesis. University of Cambridge.
Cahn, J.W., Hilliard, J.E., 1958. Free energy of a nonuniform system. I. Interfacial free energy. J. Chem. Phys. 28, 258–267.
Cárdenas, H., Mejía, A., 2016. Phase behaviour and interfacial properties of ternary system CO_2 + n-butane + n-decane: Coarse-grained theoretical modelling and molecular simulations. Mol. Phys. 114, 2627–2640.
Chunxi, L., Wenchuan, W., Zihao, W., 2000. A surface tension model for liquid mixtures based on the Wilson equation. Fluid Phase Equilib. 175, 185–196.
Connors, K.A., Mecozzi, S., 2010. Surfaces and Interfaces. John Wiley & Sons, pp. 201–208.
Connors, K.A., Wright, J.L., 1989. Dependence of surface tension on composition of binary aqueous-organic solutions. Anal. Chem. 61, 194–198.
Cornelisse, P.M.W., Peters, C.J., de Swaan Arons, J., 1993. Application of the Peng-Robinson equation of state to calculate interfacial tensions and profiles at vapour-liquid interfaces. Fluid Phase Equilib. 82, 119–129.
Cumicheo, C., Cartes, M., Müller, E.A., Mejía, A., 2018. Experimental measurements and theoretical modeling of high-pressure mass densities and interfacial tensions of carbon dioxide + n-heptane + toluene and its carbon dioxide binary systems. Fuel 228, 92–102.
Daehwan, J., Dongjo, K., Jooho, M., 2009. Influence of fluid physical properties on ink-jet printability. Langmuir 25, 2629–2635.
Design Institute for Physical Properties, 2019. Sponsored by AIChE., DIPPR Project 801 - Full Version.
Diddens, C., Tan, H., Lv, P., Versluis, M., Kuerten, J.G.M., Zhang, X., Lohse, D., 2017. Evaporating pure, binary and ternary droplets: thermal effects and axial symmetry breaking. J. Fluid Mech. 823, 470–497.
Enders, S., Kahl, H., 2008. Interfacial properties of water + alcohol mixtures. Fluid Phase Equilib. 263, 160–167.
Eötvös, R., 1886. Ueber den Zusammenhang der Oberflächenspannung der Flüssigkeiten mit ihrem Molecularvolumen. Ann. Phys. 263, 448–459.
Escobedo, J., Mansoori, G.A., 1998. Surface-tension prediction for liquid mixtures. AIChE J. 44, 2324–2332.
Eslami, F., Elliott, J.A.W., 2013. Design of microdrop concentrating processes. J. Phys. Chem. B 117, 2205–2214.
Eslami, F., Elliott, J.A.W., 2014. Role of precipitating solute curvature on microdrops and nanodrops during concentrating processes: The nonideal Ostwald–Freundlich equation. J. Phys. Chem. B 118, 14675–14686.
Eslami, F., Elliott, J.A.W., 2014b. Stability analysis of microdrops during concentrating processes. J. Phys. Chem. B 118, 3630–3641.
Fanchi, J.R., 2007. Calculation of parachors for compositional simulation: an update. SPE Reserv. Eng. 5, 433–436.
Firoozabadi, A., 2016. Thermodynamics and Applications in Hydrocarbon Energy Production. McGraw-Hill Education.
Garrido, J.M., Polishuk, I., 2018. Toward development of a universal CP-PC-SAFT-based modeling framework for predicting thermophysical properties at reservoir conditions: Inclusion of surface tensions. Indust. Eng. Chem. Res. 57, 8819–8831.
Gloor, G.J., Jackson, G., Blas, F.J., Martín Del Río, E., De Miguel, E., 2007. Prediction of the vapor–liquid interfacial tension of nonassociating and associating fluids with the SAFT-VR density functional theory. J. Phys. Chem. C 111, 15513–15522.
Guggenheim, E.A., 1945. The principle of corresponding states. J. Chem. Phys. 13, 253–261.
Heidemann, R.A., Khalil, A.M., 1980. The calculation of critical points. AIChE J. 26, 769–779.
Herrmann, L., 1994. Untersuchung von Struktur und Grenzflächeneigenschaften binärer Systeme, Ph.D. thesis, Martin-Luther-Universität Halle-Wittenberg.
Hsu, J.J.-C., Nagarajan, N., Robinson, R.L., 1985. Equilibrium phase compositions, phase densities, and interfacial tensions for CO_2 + hydrocarbon systems. 1. CO_2 + n-butane. J. Chem. Eng. Data 30, 485–491.
Jaeger, P.T., Alotaibi, M.B., Nasr-El-Din, H.A., 2010. Influence of compressed carbon dioxide on the capillarity of the gas–crude oil–reservoir water system. J. Chem. Eng. Data 55, 5246–5251.
Jin, Z., Firoozabadi, A., 2016. Thermodynamic modeling of phase behavior in shale media. SPE J., 190–207
Jufu, F., Buqiang, L., Zihao, W., 1986. Estimation of fluid-fluid interfacial tensions of multicomponent mixtures. Chem. Eng. Sci. 41, 2673–2679.
Karbowiak, T., Debeaufort, F., Voilley, A., 2006. Importance of surface tension characterization for food, pharmaceutical and packaging products: a review. Crit. Rev. Food Sci. Nutr. 46, 391–407.
Kharin, S.E., Kniga, A.A., Sorokina, G.S., 1968. Surface tension of water–ethanol–methanol solutions. Izvestiya Vysshikh Uchebnykh Zavedenii Khimiya i Khimicheskaya Tekhnologiya 12, 1341–1344.
Kim, H., Stone, H.A., 2018. Direct measurement of selective evaporation of binary mixture droplets by dissolving materials. J. Fluid Mech. 850, 769–783.
Klink, C., Planková, B., Gross, J., 2015. Density functional theory for liquid–liquid interfaces of mixtures using the perturbed-chain polar statistical associating fluid theory equation of state. Indust. Eng. Chem. Res. 54, 4633–4642.
Koch, K., Dew, B., Corcoran, T.E., Przybycien, T.M., Tilton, R.D., Garoff, S., 2011. Surface tension gradient driven spreading on aqueous mucin solutions: A possible route to enhanced pulmonary drug delivery. Mol. Pharm. 8, 387–394.
Konobeev, B., Lyapin, V., 1970. Density, viscosity, and surface tension of some binary systems. Zh. Prikl. Khim. 43, 803.
Kuchma, A.E., Shchekin, A.K., 2019. Multicomponent condensation on the nucleation stage. J. Chem. Phys. 150, 054104.
Lam, V.T., Benson, G.C., 1970. Surface tension of binary liquid systems I. Mixtures of nonelectrolytes. Can. J. Chem. 48, 3773–3781.
Larsen, P.M., Maribo-Mogensen, B., Kontogeorgis, G.M., 2016. A collocation method for surface tension calculations with the density gradient theory. Fluid Phase Equilib. 408, 170–179.
Le Brun, P.P.H., de Boer, A.H., Heijerman, H.G.M., Frijlink, H.W., 2000. A review of the technical aspects of drug nebulization. Pharm. World Sci. 22, 75–81.
Lee, H.H., Chou, K.S., Huang, K.C., 2005. Inkjet printing of nanosized silver colloids. Nanotechnology 16, 2436–2441.
Li, Z., Firoozabadi, A., 2009. Interfacial tension of nonassociating pure substances and binary mixtures by density functional theory combined with Peng–Robinson equation of state. J. Chem. Phys. 130, 154108.

Liang, X., Michelsen, M.L., Kontogeorgis, G.M., 2016. A density gradient theory based method for surface tension calculations. Fluid Phase Equilib. 428, 153–163.
Lin, H., Duan, Y.Y., Zhang, J.T., 2008. Simplified gradient theory modeling of the surface tension for binary mixtures. Int. J. Thermophys. 29, 423–433.
Liu, X., Wang, L., Qiao, Y., Sun, X., Ma, S., Cheng, X., Qi, W., Huang, W., Li, Y., 2018. Adhesion of liquid food to packaging surfaces: mechanisms, test methods, influencing factors and anti-adhesion methods. J. Food Eng. 228, 102–117.
Llovell, F., Galindo, A., Blas, F.J., Jackson, G., 2010. Classical density functional theory for the prediction of the surface tension and interfacial properties of fluids mixtures of chain molecules based on the statistical associating fluid theory for potentials of variable range. J. Chem. Phys. 133, 024704.
Luengo, G., Aracil, J., Rubio, R.G., Diaz Pena, M., 1988. Bulk and surface thermodynamic properties in mixtures of small rigid molecules: The carbon tetrachloride + carbon disulfide system. J. Phys. Chem. 92, 228–234.
Macleod, D.B., 1923. On a relation between surface tension and density. Trans. Faraday Soc. 19, 38–41.
Massoudi, R., King, A.D., 1975. Effect of pressure on the surface tension of n-hexane. adsorption of low molecular weight gases on n-hexane at 25 °. J. Phys. Chem. 79, 1676–1679.
Michelsen, M.L., 1984. Calculation of critical points and phase boundaries in the critical region. Fluid Phase Equilib. 16, 57–76.
Miqueu, C., Mendiboure, B., Graciaa, C., Lachaise, J., 2004. Modelling of the surface tension of binary and ternary mixtures with the gradient theory of fluid interfaces. Fluid Phase Equilib. 218, 189–203.
Miqueu, C., Mendiboure, B., Graciaa, A., Lachaise, J., 2005. Modeling of the surface tension of multicomponent mixtures with the gradient theory of fluid interfaces. Indust. Eng. Chem. Res, 3321–3329.
Miqueu, C., Mendiboure, B., Graciaa, A., Lachaise, J., 2008. Petroleum mixtures: An efficient predictive method for surface tension estimations at reservoir conditions. Fuel 87, 612–621.
Miqueu, C., Míguez, J.M., Piñeiro, M.M., Lafitte, T., Mendiboure, B., 2011. Simultaneous application of the gradient theory and monte carlo molecular simulation for the investigation of methane/water interfacial properties. J. Phys. Chem. B 115, 9618–9625.
Mulero, A., Cachadiña, I., Parra, M.I., 2012. Recommended correlations for the surface tension of common fluids. J. Phys. Chem. Ref. Data 41, 043105.
Nagarajan, N., Gasem, K.A., Robinson, R.L., 1990. Equilibrium phase compositions, phase densities, and interfacial tensions for CO_2 + hydrocarbon systems. 6. CO_2 + n-butane + n-decane. J. Chem. Eng. Data 35, 228–231.
Neyt, J.C., Wender, A., Lachet, V., Ghoufi, A., Malfreyt, P., 2013. Molecular modeling of the liquid-vapor interfaces of a multi-component mixture: prediction of the coexisting densities and surface tensions at different pressures and gas compositions. J. Chem. Phys. 139, 024701.
Nilssen, H.N., 2008. Calculation of Interfacial Tension of Methane + n-Butane Mixture with Gradient Theory near Critical Conditions, Technical Report, Norwegian University of Science and Technology, 2008. Report prepared for KP8108 Advanced Thermodynamics.
Niño Amézquita, O.G., Enders, S., Jaeger, P.T., Eggers, R., 2010. Measurement and prediction of interfacial tension of binary mixtures. Indust. Eng. Chem. Res. 49, 592–601.
Niño Amézquita, O.G., Enders, S., Jaeger, P.T., Eggers, R., 2010. Interfacial properties of mixtures containing supercritical gases. J. Supercrit. Fluids 55, 724–734.
Ozturk, T., Erbil, H.Y., 2018. Evaporation of water-ethanol binary sessile drop on fluoropolymer surfaces: Influence of relative humidity. Colloids Surf., A 553, 327–336.
Peng, D.-Y., Robinson, D.B., 1976. A new two-constant equation of state. Indust. Eng. Chem. Fundamentals 15, 59–64.
Peng, D.-Y., Robinson, D.B., 1977. A rigorous method for predicting the critical properties of multicomponent systems from an equation of state. AIChE J. 23, 137–144.
Pennington, B., Hough, E., 1965. Interfacial tension of the methane–normal butane system. Producers Month. 29, 4.
Pereira, L.M., Chapoy, A., Burgass, R., Tohidi, B., 2016. Measurement and modelling of high pressure density and interfacial tension of (gas + n-alkane) binary mixtures. J. Chem. Thermodyn. 97, 55–69.
Robinson, D., Peng, D., 1978. Research report 28: The characterization of the heptanes and heavier fractions for the GPA Peng-Robinson programs. Gas Process. Assoc.
Sahimi, M., Taylor, B.N., 1991. Surface tension of binary liquid–vapor mixtures: a comparison of mean-field and scaling theories. J. Chem. Phys. 95, 6749–6761.
Sandoval, D.R., Yan, W., Michelsen, M.L., Stenby, E.H., 2016. The phase envelope of multicomponent mixtures in the presence of a capillary pressure difference. Indust. Eng. Chem. Res. 55, 6530–6538.
Sarman, S., Greberg, H., Satherley, J., Penfold, R., Nordholm, S., 2000. Effective potential approach to bulk thermodynamic properties and surface tension of molecular fluids. II. Binary mixtures of n-alkanes and miscible gas. Fluid Phase Equilib. 172, 145–167.
Schechter, D., Guo, B., 2007. Parachors based on modern physics and their uses in IFT prediction of reservoir fluids. SPE Reserv. Eval. Eng. 1, 207–217.
Schmidt, R.L., Randall, J.C., Lawrence Clever, H., 1966. The surface tension and density of binary hydrocarbon mixtures: Benzene–n-hexane and benzene–n-dodecane. J. Phys. Chem. 70, 3912–3916.
Seneviratne, K.N., Hughes, T.J., Johns, M.L., Marsh, K.N., May, E.F., 2017. Surface tension and critical point measurements of methane + propane mixtures. J. Chem. Thermodyn. 111, 173–184.
Shardt, N., Elliott, J.A.W., 2016. Thermodynamic study of the role of interface curvature on multicomponent vapor–liquid phase equilibrium. J. Phys. Chem. A 120, 2194–2200.
Shardt, N., Elliott, J.A.W., 2017. A model for the surface tension of dilute and concentrated binary aqueous mixtures as a function of composition and temperature. Langmuir 33, 11077–11085.
Shardt, N., Elliott, J.A.W., 2018. Isobaric vapor–liquid phase diagrams for multicomponent systems with nanoscale radii of curvature. J. Phys. Chem. B 122, 2434–2447.
Sherafati, M., Jessen, K., 2017. Stability analysis for multicomponent mixtures including capillary pressure. Fluid Phase Equilib. 433, 56–66.
Shereshefsky, J.L., 1967. A theory of surface tension of binary solutions. J. Colloid Interface Sci. 24, 317–322.
Shim, J.-U., Cristobal, G., Link, D.R., Thorsen, T., Jia, Y., Piattelli, K., Fraden, S., 2007. Control and measurement of the phase behavior of aqueous solutions using microfluidics. J. Am. Chem. Soc. 129, 8825–8835.
Stegemeier, G.L., Pennington, B.F., Brauer, E.B., Hough, E.W., 1962. Interfacial tension of the methane–normal decane system. SPE J. 2, 257–260.
Stradi, B.A., Brennecke, J.F., Kohn, J.P., Stadtherr, M.A., 2001. Reliable computation of mixture critical points. AIChE J. 47, 212–221.
Talreja, M., Kusaka, I., Tomasko, D.L., 2012. Analyzing surface tension in higher alkanes and their CO_2 mixtures. Fluid Phase Equilib. 319, 67–76.
Tan, S.P., Piri, M., 2015a. Equation-of-state modeling of associating-fluids phase equilibria in nanopores. Fluid Phase Equilib. 405, 157–166.
Tan, S.P., Piri, M., 2015b. Equation-of-state modeling of confined-fluid phase equilibria in nanopores. Fluid Phase Equilib. 393, 48–63.
Tang, X., Gross, J., 2010. Density functional theory for calculating surface tensions with a simple renormalization formalism for the critical point. J. Supercrit. Fluids 55, 735–742.
Teixeira, P.I.C., Almeida, B.S., Telo da Gama, M.M., Rueda, J.A., Rubio, R.G., 1992. Interfacial properties of mixtures of molecular fluids: Comparison between theory and experiment; methyl iodide + carbon tetrachloride and acetonitrile + carbon tetrachloride. J. Phys. Chem. 96, 8488–8497.
Van der Waals, J.D., 1979. The thermodynamic theory of capillarity under the hypothesis of a continuous variation of density. Verhandel. Konink. Akad. Weten. Amsterdam 1.8 (1893). J. Stat. Phys. 20, 197–200.
Wang, L., Parsa, E., Gao, Y., Ok, J.T., Neeves, K., Yin, X., Ozkan, E., 2014. Experimental study and modeling of the effect of nanoconfinement on hydrocarbon phase behavior in unconventional reservoirs. In: SPE Western North American and Rocky Mountain Joint Meeting, Society of Petroleum Engineers.
Ward, C.A., Balakrishnan, A., Hooper, F.C., 1970. On the thermodynamics of nucleation in weak gas–liquid solutions. J. Basic Eng. 92, 695–701.
Warren, H.G., Hough, E.W., 1970. Interfacial tension of the methane–normal heptane system. SPE J. 10, 327.
Weinaug, C.F., Katz, D.L., 1943. Surface tensions of methane-propane mixtures. Indust. Eng. Chem. 35, 239–246.
Wohlfarth, C., Wohlfarth, B., 1997. Binary Mixtures: Data. Springer.
Wu, T., Hirata, K., Suzuki, H., Xiang, R., Tang, Z., Yomo, T., 2012. Shrunk to femtolitre: Tuning high-throughput monodisperse water-in-oil droplet arrays for ultra-small micro-reactors. Appl. Phys. Lett. 101, 2–6.
Yu, Y.S., Sun, L., Huang, X., Zhou, J.Z., 2019. Evaporation of ethanol/water mixture droplets on a pillar-like PDMS surface. Colloids Surf., A 574, 215–220.
Zhu, J.Y., Duan, Y.Y., Yang, Z., Lin, H., 2014. Factors influencing the surface tension of binary hydrocarbon mixtures. Fuel 116, 116–122.
Zuo, Y.-X., Stenby, E.H., 1998. Prediction of interfacial tensions of reservoir crude oil and gas condensate systems. SPE J., 134–145